Design criteria for Fiber Reinforced Rubber Bearings

J. M. Kelly
Earthquake Engineering Research Center
University of California, Berkeley

A. Calabrese & G. Serino
Department of Structural Engineering
University of Naples Federico II

SUMMARY:
This paper contains the findings of a study on the mechanical behaviour of unbonded Fiber-Reinforced Bearings (FRB). Typical FRBs consist of several layers of rubber that are bonded to fiber reinforcing sheets. The purpose of the reinforcement is to prevent the rubber from bulging laterally under compressive load. The most important aspects of these bearings are (i) they do not have thick end plates; (ii) they are not bonded to the top and bottom support surfaces; and (iii) their reinforcements are very flexible. These aspects may seem to be design deficiencies, but they have the advantage of eliminating the presence of tensile stresses in the bearing by allowing it to roll off the supports when it is sheared. This reduces the typical bonding requirements. The weight and the cost of isolators is reduced by using fiber reinforcing, no end-plates and no bonding to the support surfaces, offering a low-cost lightweight isolation system. The paper introduces simple theories, valid as design criteria, for the determination of the tensile stresses in the reinforcement, the vertical stiffness of the bearing, the ultimate lateral displacement. A good benchmark to test the theories is proposed in this work using the output of Finite Element Analysis (FEA).

Keywords: Low-Cost Fiber Reinforced Isolators, Design Criteria, FEA

1. INTRODUCTION

Modern seismic protection systems have shown their good performance in past earthquakes, for example in the 2011 off the Pacific coast of Tohoku Earthquake on March 11, 2011. Among the different available techniques, seismic isolation seems to be the most applicable for a large range of structures. Generally, an isolation bearing consists of thin sheets of rubber bonded to steel plates. The system has enough vertical rigidity to sustain gravitational load and horizontal flexibility to shift the fundamental frequency of the building away from the dominant frequency range of most earthquakes. This technique is generally applied to expensive and strategically relevant buildings. Consequently, for this kind of applications, devices are large, expensive and heavy.
In order to ensure the diffusion of base isolation to common residential buildings, especially in earthquake prone areas in developing countries, a reduction of the cost and weight of the devices is required. The possibility of replacing the steel reinforcing plates in the bearing with fiber reinforcement is presented in this paper.
A fiber reinforcement is not only lighter than steel but it allows a less labour-intensive manufacturing process that would reduce production cost. This paper focuses on the behaviour of Fiber Reinforced Bearings (FRBs) under pure compression and shear introducing references for sizing low cost devices.

2. BEHAVIOUR UNDER COMPRESSION

2.1. Vertical stiffness and stress in the reinforcement

The essential characteristic of an elastomeric isolator is the very large ratio of the vertical stiffness to the horizontal stiffness. This ratio can be in the order of magnitude of hundreds. In the case of FRBs, this large ratio is due to the fiber sheets which allow the rubber to shear freely while preventing its

lateral bulging.
For design purposes, it is particularly important to predict the vertical stiffness and the collapse condition of FRBs under compression.
Under compression, collapse of the bearing can occur for global failure due to buckling of the device, local ruptures of the reinforcement or the detachment of the rubber from the fiber sheets.
Therefore, an accurate knowledge of the global characteristics of the device and of the stress distributions at the rubber fiber interfaces and in the fiber reinforcement is necessary.
To predict the compression stiffness of thin elastomeric pad a linear elastic theory is used.
The first analyses of the compression stiffness for rigid reinforcement were done by Rocard (1973), Gent and Lindley (1959), and Gent and Meinecke (1970). Further developments in the study of traditional elastomeric bearings were made by Kelly and Takhirov (2002) using a simplified version of the previous theories. Tsai and Kelly (2001) also extended the theoretical results to the analysis of fiber-reinforced elastomeric isolators developing an approximate closed-form solution (the pressure solution) based on several assumptions.
The kinematic assumptions are as follows:

(i) points on a vertical line before deformation lie on a parabola after loading,
(ii) horizontal planes remain horizontal, and
(iii) the reinforcement stretching produces a constant displacement trough the thickness.

Furthermore, rubber is assumed incompressible, and the pressure is assumed to be the dominant stress component.
For simplicity we consider the solution for a long rectangular strip pad of thickness t in which a rectangular Cartesian coordinate system, (x,y,z), is located in the middle surface of the pad, as shown in Fig.2.1.

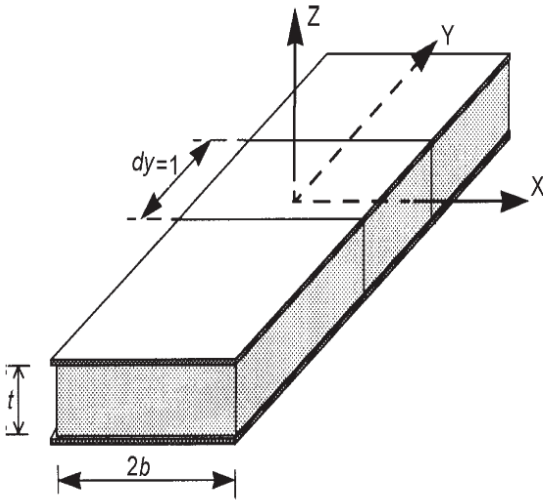

Figure 2.1. Infinitely long rectangular pad showing dimensions

In the previous hypothesis, the pressure solution gives the stress in the reinforcement, $F(x)$, and the effective compressive modulus, E_c:

$$F(x) = \frac{\Delta}{t} E_f t_f \left(1 - \frac{\cosh \alpha x / b}{\cosh \alpha}\right) \tag{2.1}$$

$$E_c = \frac{E_f t_f}{t}\left(1 - \frac{\tanh \alpha}{\alpha}\right) \tag{2.2}$$

In which

$$\alpha^2 = 12Gb^2 / E_f t_f t \tag{2.3}$$

where:

- Δ is the vertical displacement,
- E_f is the elastic modulus of the reinforcement,
- t_f is the thickness of the reinforcement,
- G is the shear modulus of the rubber,
- $B = 2b$ is the base length of the bearing.

When $\alpha \to 0$, i.e. , $E_f \to \infty$, imposing $S = b/2t_r$, E_c becomes $E_c = 4GS^2$. This result is the same that can be derived applying the pressure solution to bearings with rigid reinforcement. The formula also shows that $E_c < 4GS^2$ for all the values of E_f. Once E_c, the instantaneous compression modulus of fiber-rubber composite under a specified level of vertical load, is known the vertical stiffness of a bearing can be easily computed as $K_V = (E_c A)/t_r$ where A is the area of the bearing and t_r is the total thickness of rubber in the device.

The pressure solution can be applied even for compressible material. In case strip type bearings, the solution of the problem is

$$E_c = K \frac{\beta^2}{\alpha^2 + \beta^2}\left(1 - \frac{\tanh \lambda}{\lambda}\right) \tag{2.4}$$

where K is the bulk modulus of the rubber, $\beta^2 = 12Gb^2 / Kt^2$ and $\lambda^2 = \alpha^2 + \beta^2$.

2.2. Theoretical results

According to the previous solution Eqns. 2.1-2.4 we can determine the vertical stiffness of strip type FRB bearings, K_V ,and the tensile stress in the reinforcement, $\sigma_f(x)$. In Table 2.1 some calculation examples are reported for bearings with different shape factors, S. The different values of shape factor are obtained by increasing the values of the base of the device (B= 250; 300; 350; 400; 450; 500mm). Results are referred to bearings with a longitudinal dimension of 750mm. As shown in Fig.2.1, each device is made of twenty-eight rubber layers with twenty-nine interleaf fiber sheets. Each rubber layer is t_r = 6.36 mm thick, and each fiber sheet is t_f = 0.07 mm thick.

Table 2.1. Applications of the pressure solution.

GEOMETRICAL AND MECHANICAL PROPERTIES							
B	[mm]	250	300	350	400	450	500
H	[mm]	180					
L	[mm]	750					
t_f	[mm]	0.07					
n	[-]	29 fiber layers					
tr	[mm]	6.37					
Ef	[MPa]	14000					
G	[MPa]	0.70					

COMPRESSION OF PAD WITH RIGID REINFORCEMENT							
E_c	[Mpa]	1082.93	1559.42	2122.54	2772.30	3508.69	4331.72
K_v	[N/mm]	1140919	1971509	3130683	4673206	6653842	9127356

COMPRESSION STIFFNESS WITH COMPRESSIBILITY OF THE ELASTOMER (K=2000MPa)							
β	[-]	1.27	1.53	1.78	2.04	2.29	2.55
E_c	[MPa]	658.29	809.58	940.60	1051.90	1145.77	1224.92
K_v	[N/mm]	693539	1023520	1387352	1773163	2172814	2581018
COMPRESSION STIFFNESS WITH FLEXIBLE REINFORCEMENT							
α	[-]	4.59	5.51	6.43	7.34	8.26	9.18
E_c	[Mpa]	120.60	126.19	130.19	133.19	135.52	137.39
K_v	[N/mm]	127059	159541	192028	224515	257003	289491
FLEXIBLE REINFORCEMENT AND COMPRESSIBILITY(K=2000MPa)							
λ	[-]	4.76	5.72	6.67	7.62	8.58	9.53
E_c	[Mpa]	113.10	118.11	121.69	124.37	126.45	128.12
K_v	[N/mm]	119160	149319	179481	209643	239806	269969

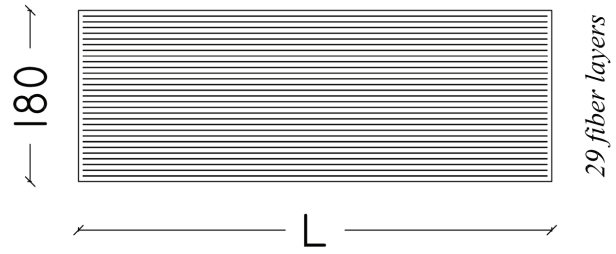

Figure 2.1 Cross section of a bearing

2.3. FEA results

The goal of this section is to verify the validity of the results provided by the pressure solution by comparing them with results from FEA.

A series of FEA of rectangular elastomeric bearings were conducted using the general-purpose finite element program MSC.Marc 2005 [MSC.Software 2004]. The analyses were performed using a two-dimensional model under the plane strain assumption assuming specialized element types that automatically address numerical issues to get accurate solutions to large strain problems, change of contact conditions, sliding and near-incompressibility of the rubber.

The results of analysis presented in this paper are based on the widely popular mixed method proposed by Herrmann (1965). A restricted case of the general Hellinger-Reissner variational principle is used to derive the stiffness equations.

The finite element discretization consists of square four-node elements with side length of 2 mm and is denser at the contact interface.

The fiber reinforcement of the bearing is modeled using the rebar element. It is a tension element of a liner elastic isotropic material with Young's modulus E = 14000MPa, and thickness t_f = 0.07mm.

The rubber is modelled by a single-parameter Mooney-Rivlin material (i.e., Neo-Hookean) with strain energy function that is described by the shear modulus G = 0.7 MPa, and the bulk modulus κ = 2000 MPa.

The top and bottom support surfaces are modeled as rigid lines. The contact between the rubber and the support surfaces is modeled by Coulomb friction with μ = 0.9. As mentioned above, the analysis is carried out under the plane strain assumption. Moreover, large strain theory is employed. The kinematics of deformation is described following the Updated Lagrangian formulation (i.e., the Lagrangian frame of reference is redefined at the last completed iteration of the current increment). Furthermore, Full Newton-Raphson solution method is used.

The bearings are loaded in two steps:

1) Pure compression [0-3.45MPa]
2) Horizontal displacement is increased till collapse (= Δ_u).

Figures 2.2 and 2.3 show the contour maps of the equivalent stress obtained from analysis with Marc for bearings 250 and 500 under pure compression

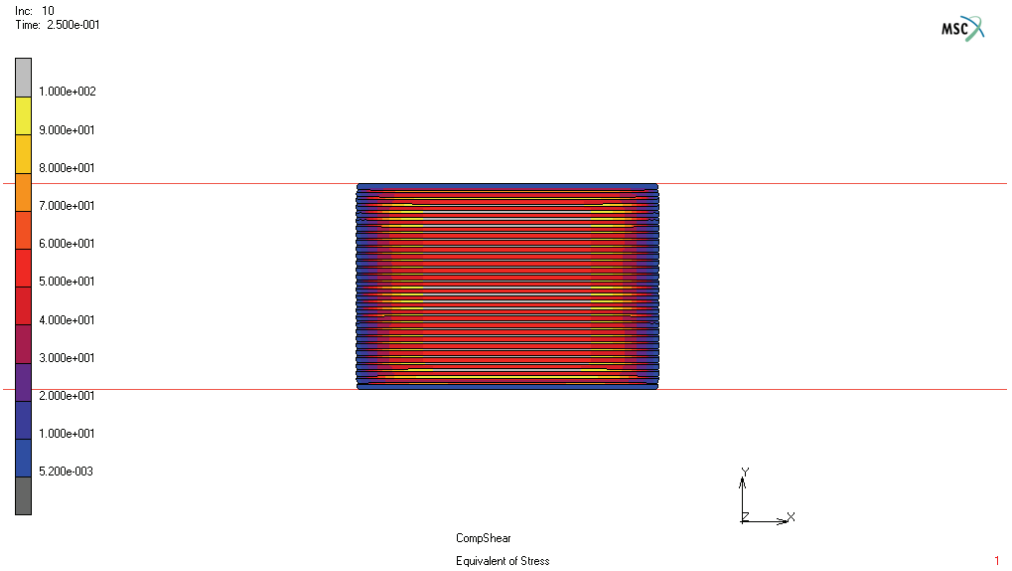

Figure 2.2. Von Mises stress contours [MPa] at peak vertical force in a bearing of base B=250mm

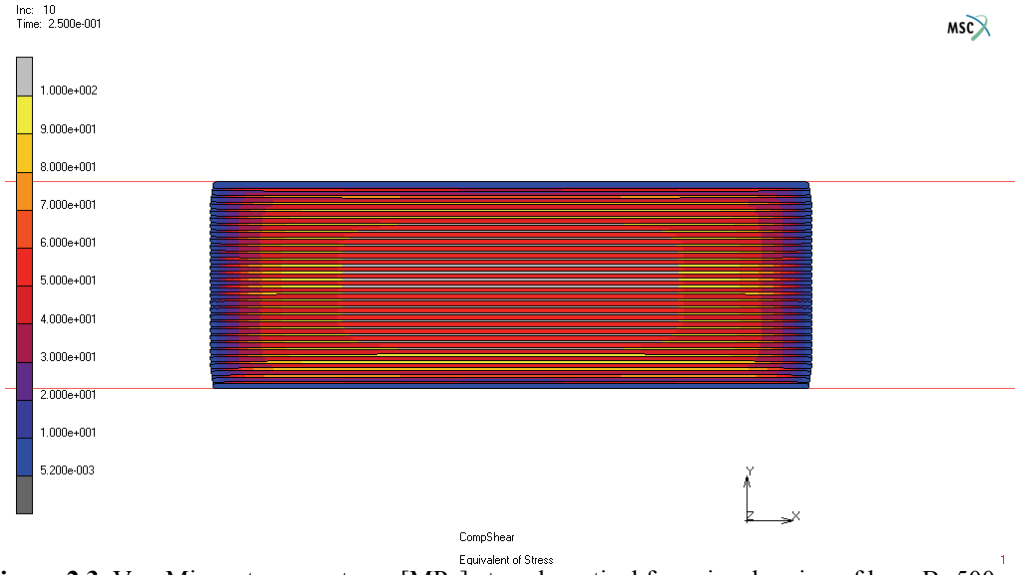

Figure 2.3. Von Mises stress contours [MPa] at peak vertical force in a bearing of base B=500mm

The contours show a stress concentration in the core of the bearings. For a given compressive force P (average pressure $= P/A$ =3.45 MPa) in the considered range of bases, the maximum equivalent stress in the core of the bearing is unaffected by the change of the dimension of the device. Therefore, the stress in the core of the bearing is the same when the base dimension is modified. However, as expected, a new arrangement of stress distribution along the base length can be observed when the dimensions are changed. As a result, for bigger bearings as we move towards the free edges, the stress drops less aggressively than for smaller ones.

It is worth noting that due to the frictional restraint of the supports, the fiber layers closest to the supports are in compression.

Fig.2.4 is a plot of the vertical stiffness as a function of the shape factor for the six bearings of different geometry.

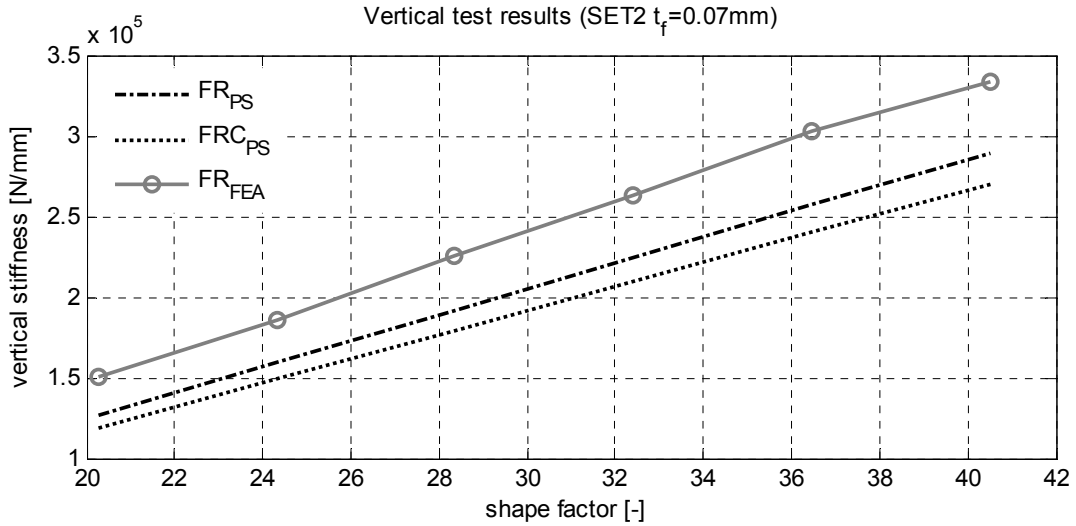

Figure 2.4. Vertical stiffness Vs. shape factor

FR_{PS} and FRC_{PS} are the theoretical vertical stiffness results of fiber reinforced bearings for incompressible and compressible material respectively. The FEA outputs are plotted as FR_{FEA}.

FEA and pressure solution output result in good agreement. FEA gives higher values of vertical stiffness because of a stiffening contribution of the quadratic mesh.

Fig. 2.5 shows the plot of tensile stress as a function of the dimensionless length of the device, x/B, for the mid-height fiber layer, where the stresses are the largest. In the figure, the solid line represents the PS result and the dotted line represent the FEA result.

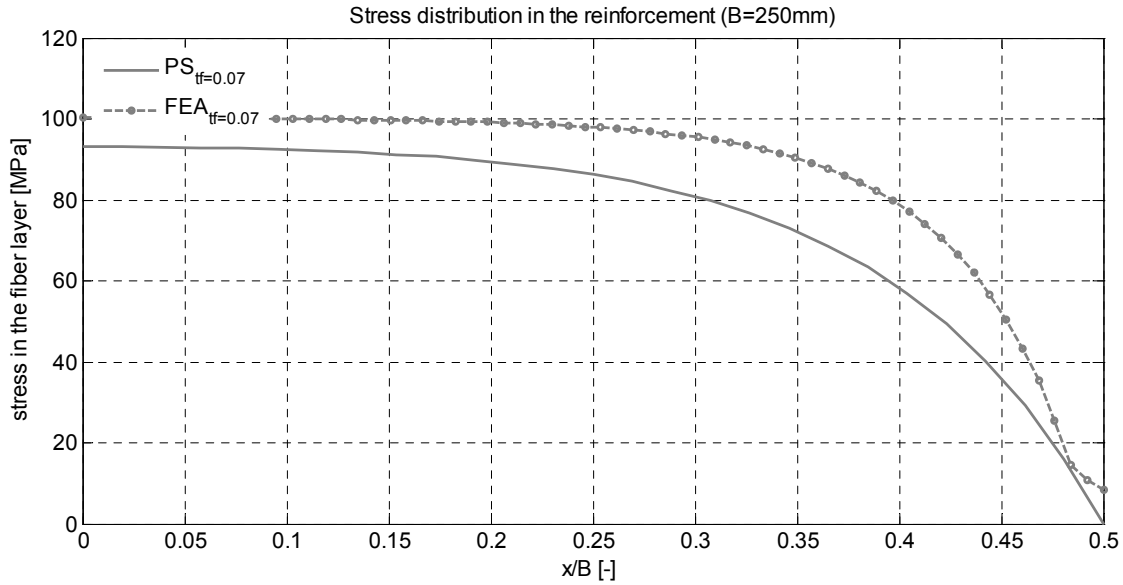

Figure 2.5. Stress distribution in the reinforcement (FEA VS. Pressure Solution)

The pressure solution gives accurate results for the description of the stress of the fiber in the bearing's core. Towards the free edges of the bearings, for a length of 10% of the base, the FE and the PS results are different. This difference is very low for higher shape factor but is significant as the shape factor decreases.

3. STABILITY OF HORIZONTAL DISPLACEMENT

3.1. Design criterion

The basic premise for the analysis of these bearings is that the regions of the bearing that have rolled off the rigid supports are free of all stress and that the volume under the contact area has constant shear stress. Under this assumption, the active area that produces the force of resistance F to displacement Δ, is $B-\Delta$ and thus the force (per unit width of the bearing) is $F=G\gamma\left(B-\Delta\right)$, but $\gamma=\Delta/t_r$, thus $F=G\left(B-\Delta\right)\Delta/t_r$, and consequently the force displacement curve has zero slope when

$$\frac{dF}{d\Delta}=\frac{G}{t_r}\left(B-2\Delta\right)=0, \quad \text{i.e., when } \Delta=B/2 \tag{3.1}$$

The implication of this result is that the bearing remains stable in the sense of positive tangential force-displacement relationship so long as the displacement is less than half the length in the direction of the displacement. As a result of the limiting displacement analysis, it is possible to determine a simple design criterion for this type of bearing. We need only to determine a maximum required design displacement which normally would depend on the site, the anticipated isolation period and damping. If we denote this by Δ then the requirement for positive incremental horizontal stiffness requires that the width B of the bearing in the direction of the displacement be at least twice the displacement, i.e. $B\geq 2\Delta$.

3.2. FEA Shear Results

In the second part of the analysis, a constant vertical load is applied, and then the horizontal displacement is increased in order to investigate the ultimate behavior of the bearings.
Figures 3.1 is a Von Mises stress contour map for B=250 at the displacement that corresponds to the peak force in the load-displacement curve.

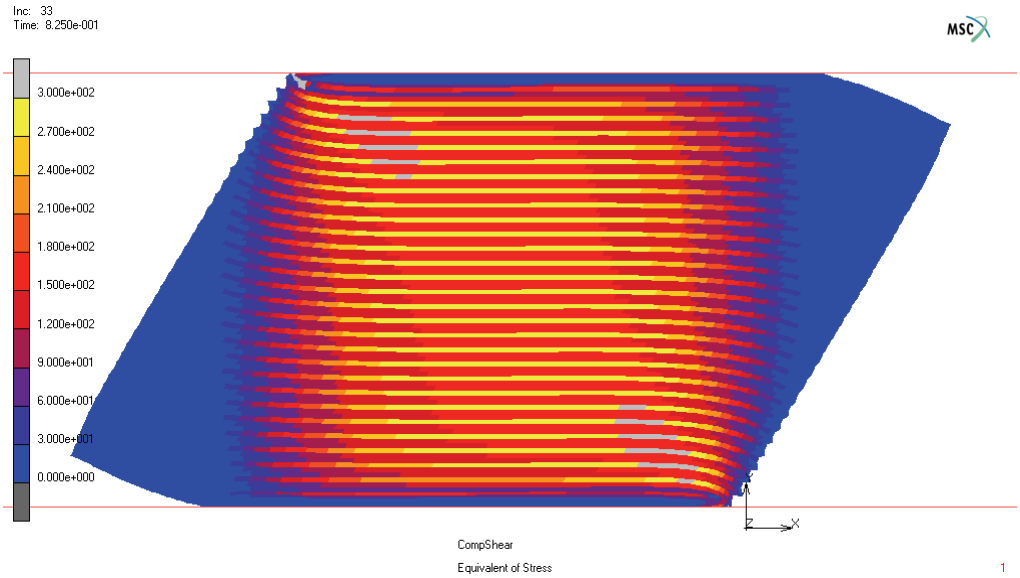

Figure 3.1 Von Mises stress contours [MPa] at peak horizontal force in a bearing of base B=250mm

The aforementioned figure clearly shows the favourable response of an isolator which is not bonded to the top or bottom supports. This is due to the elimination of tension in the elastomer. In a bonded bearing under the simultaneous action of shear and compression, the presence of an unbalanced moment at both top and bottom surfaces produces a distribution of tensile stresses in the triangular

region outside the overlap between top and bottom. The compression load is carried through the overlap area, and the triangular regions created by the shear displacement provide the tensile stresses to balance the moment. These tensile stresses must be sustained by the elastomer and also by the bonding between the elastomer and the steel reinforcement plates. The provision of these bonding requirements is the main reason for the high cost of current designs of isolator bearings for buildings. With the elimination of these tension stresses, the bonding requirements for this type of bearing are reduced.
Figures 3.2 is the stress contour in the reinforcement at peak horizontal force.

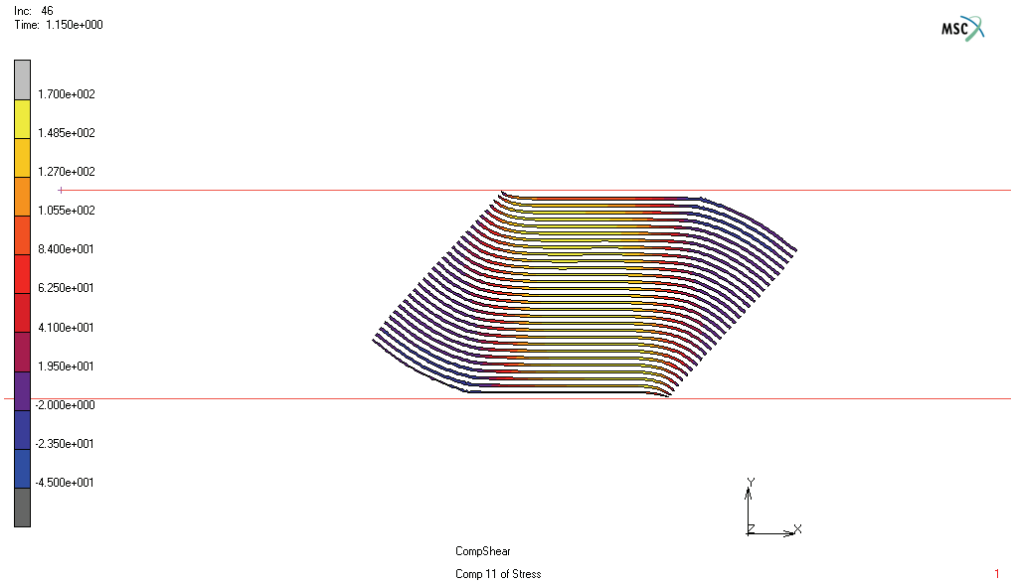

Figure 3.2 Tension contours [MPa] in the fiber reinforcement at maximum shear (B=250)

In Fig.3.3 the horizontal load is plotted as a function of the horizontal displacement for the six bearings under a vertical pressure of 3.45 MPa.

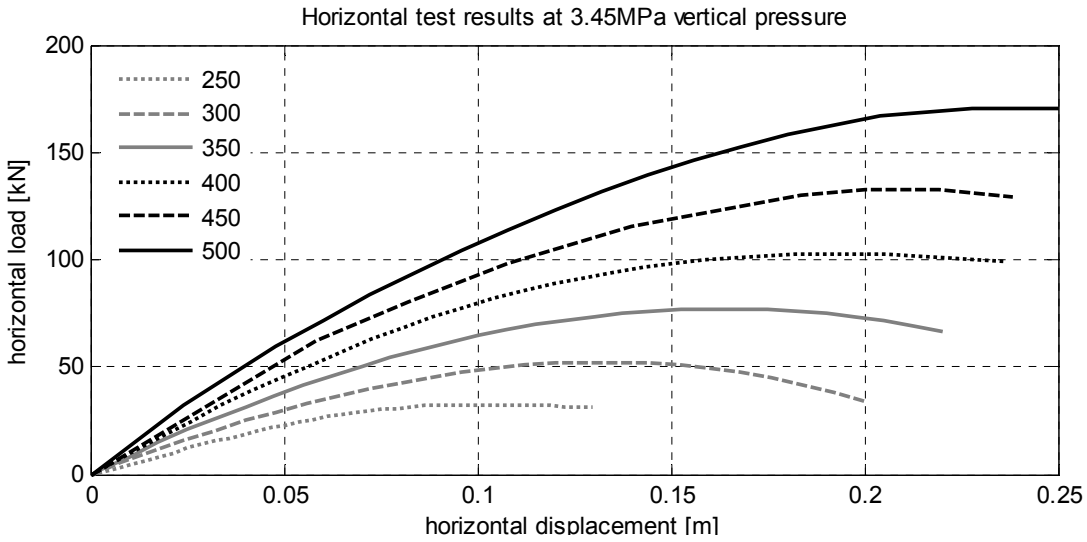

Figure 3.3 Force-displacement curves

Fig.3.4 shows the horizontal load VS the dimensionless horizontal displacement.

These curves are straight lines up to the value of the lateral load for which roll-off of the right end starts to occur. A progressive reduction of the lateral tangent stiffness is then observed with further

increase of the lateral load.
The large deformation that FRBs experience can be modeled accurately in Marc. However, the finite element mesh distorts so heavily that the analysis becomes grossly inaccurate or stops due to individual mesh elements turning inside out and pre-specified convergence criteria not being satisfied.
The values that describe the ultimate behavior are summarized in Table 3.1.

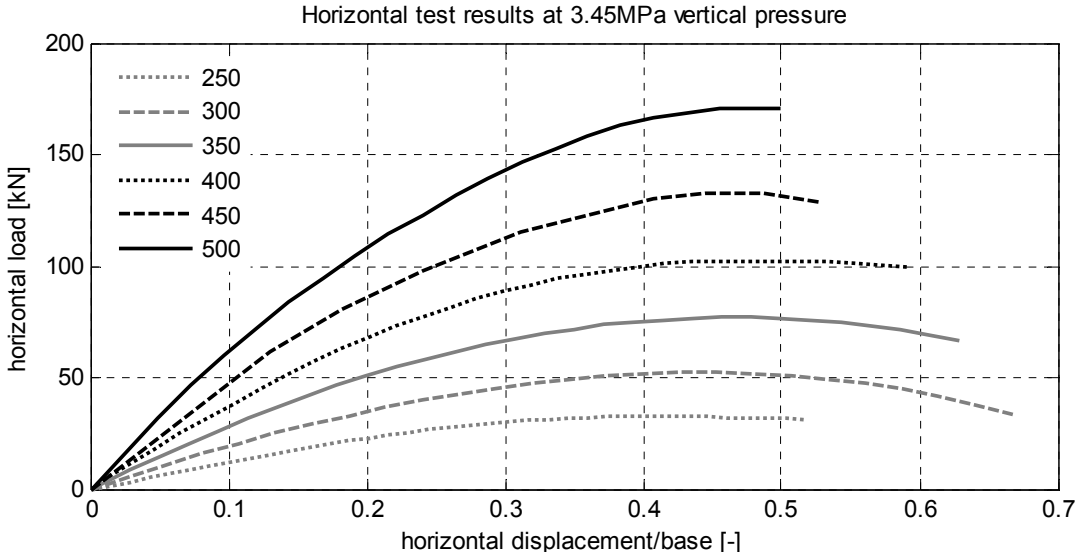

Figure 3.4 Force-displacement/base curves

Table 3.1 Ultimate performances of the bearings under horizontal load.

	B [mm]	S [-]	$F_{h,u}$ [kN]	τ_u [MPa]	Δ_u [mm]	Δ_u/B [-]	γ_u [%]
NAME	500	43.48	170.5	0.45	204	0.4	1.1
	450	39.13	139.9	0.41	195	0.4	1.1
	400	34.78	104.1	0.35	190	0.5	1.1
	350	26.09	77.17	0.29	167	0.5	0.9
	300	21.74	52.13	0.23	136	0.5	0.8
	250	43.48	32.92	0.18	104	0.4	0.6

4. CONCLUSIONS

In this study, the following observations and conclusions can be made.
The most important aspects of FRB are: they do not have thick end plates, they are not bonded to the top and bottom support surfaces, and their reinforcements are flexible. These features at first sight might seem to be deficiencies of their design, but they have the advantage to eliminate the presence of tensile stresses in the bearing by allowing it to roll off the supports. This reduces the costly stringent bonding requirements that are typical for conventional bearings.
The validity of the pressure solution, a method developed to describe the global behavior and the stress distribution in rubber bearings, and the validity of an ultimate analysis to investigate the peak horizontal displacement are discussed by comparing the theoretical results with a FEA.
Bearings with different shape factors were modelled and loaded under pure compression and shear. For both load conditions, the bearings exhibit a linear behavior under a wide range of displacement. For the theoretical and the numerical solution, in the considered range of geometries, the variation of the vertical stiffness as a function of the shape factor is linear.
The pressure solution result, except near the free edges, is particularly valid to determine the stress distribution in the reinforcement. Moreover, the resultant maximum stress in the reinforcement is in good agreement to the FE outputs.

In the considered range of dimensions, bearings with a different shape factor exhibit at peak lateral displacement, under the same vertical pressure, the same maximum stress in the reinforcement. This value is approximately three times larger than when the bearing is under pure compression.
The shear tests conducted in Marc for the different bearings show that the peak horizontal displacement is approximately half of the base length.
The theoretical model, which was useful to determine the peak horizontal displacement, gives good results even when compared against the FEA with non-zero vertical load. It was also observed that for a fixed axial load, the shear load goes through a maximum as the shear deflection is further increased. The displacement at which this maximum occurs decreases with increasing axial load.
Therefore, it can be concluded that further FEA are necessary to precisely evaluate the influence of the vertical load on the horizontal behavior of the bearings. Moreover, this study was conducted considering the shape factor S as the only variable. Analytical results showed that the shape factor is an important geometrical parameter that characterizes the mechanics of the bearings; however, there are other parameters, such as the slenderness of the bearing, that have to be taken into account to fully describe the global behavior of the device.
The comparison between the theoretical and the FEA outputs shows potential to validate further theoretical results.
Results of the theoretical model, such as the vertical stiffness, the maximum stress in the reinforcement, and the peak horizontal displacement of the bearing, are in good agreement with the results from FEA.

REFERENCES

Gent, A.N., Lindley, P.B. (1959). Compression of bounded rubber blocks, *Proceeding Institution of Mechanical Engineers*, **173**(3), 111-122.

Gent, A.N., Meinecke, E.A. (1970). Compression, bending and shear of bonded rubber blocks, *Polymer Engineering and Science*, **10** (1), 48-53.

Herrmann, L.R. (1965). Elasticity equations for incompressible and nearly incompressible materials by a variational theorem, AIAA J. **3**, pp. 1896–1900.

Kelly, J.M., Takhirov, S.M. (2002). Analytical and experimental study of fiber-reinforced bearings, *PEER 2002/11*.

Rocard, Y. (1937). Note sur le calcul des proprietes elastique des supports en caoutchouc adherent, *Journal de Physique et de Radium*, 8, 197.

Tsai, HC., Kelly, J.M. (2001). Stiffness analysis of fiber-reinforced elastomeric isolators, *PEER 2001/05.*